IEEE Access
Multidisciplinary | Rapid Review | Open Access Journal

Received February 2, 2019, accepted February 20, 2019, date of publication February 26, 2019, date of current version March 18, 2019.

Digital Object Identifier 10.1109/ACCESS.2019.2901745

Robust Localization for Cognitive IoT via the Mobile Anchor Node Based on the Diameter-Varying Spiral Line

XIN WANG[1,2], ZHIHONG QIAN[1], (Senior Member, IEEE), XUE WANG[1], AND LAN HUANG[3]

[1]College of Communication Engineering, Jilin University, Changchun 130012, China
[2]College of Information Technology, Jilin Agricultural University, Changchun 130018, China
[3]College of Computer Science and Technology, Jilin University, Changchun 130012, China

Corresponding author: Xue Wang (jluwangxue@163.com)

This work was supported in part by the Fundamental Research Funds of Jilin University under Grant SXGJQY2017-9 and Grant 2017TD-19, in part by the Jilin Provincial Science and Technology Department under Grant 20150101050JC, in part by the National Natural Science Foundation of China under Grant 61371092, Grant 61401175, and Grant 61771219, and in part by the Scientific Initiation Research Fund of Jilin Agricultural University under Grant 2015045.

ABSTRACT Research on IoT that merely aims at connecting and communicating is about to past. Thereafter, general objects should have the capability to learn, think, and understand both physical and social areas by themselves. Cognitive Internet of Things (CIoT) attempts to empower the current IoT with a ''brain'' for high-level intelligence, requiring networks to have the ability to bridge the physical and social worlds. This attempt means matching equipment and resources with people and their behavior. Therefore, accurate location information is crucial for equipment connecting to CIoT. This endeavor sets a higher requirement for the localization technology of wireless sensor networks in terms of accuracy, energy, and efficiency compared with that in the past. In this paper, we propose an efficient and accurate mobile anchor node assisted localization algorithm for WSNs based on diameter-varying spiral line (LDVSL), which broadcasts coordinates of the anchor node to assist localizing unknown sensor nodes. The proposed algorithm has two main innovations. First, we obtain the mobile anchor node position through a time and angle mechanism instead of GPS, given the unique characteristics of the diameter-varying spiral line. Second, the linear fitting method is adapted to select the key virtual node, which has the real maximum received signal strength indicator. Simulations indicate that the proposed LDVSL algorithm outperforms other similar algorithms in terms of average localization error and positionable node ratio. The simulations also show that the LDVSL is not affected by obstacles seriously and has good robustness. The LDVSL has a wide prospect of application in CIoT.

INDEX TERMS CIoT, localization, mobile anchor node, diameter-varying spiral line, linear fitting.

I. INTRODUCTION

With the rapid development of wireless communication techniques in the past few years, IoT has been widely used as a cyber physical systems in the fields of modern intelligent services such as ecological protection, smart homes, food safety, environmental, logistics, transportation, and national information coverage [1], [2]. According to the latest surveys, approximately 600 billion devices will be connected to the IoT by 2020. With the increasing interconnectivity among general things or objects, many new services or applications are emerging, generating massive data in an explosive manner [3]. However, many of the existing Internet of Things applications are still not intelligent enough to perceive data and perform decision making, and they are highly dependent on human beings for cognition processing [4]. Therefore, cognitive computing has gained the interest of IoT researchers [5]–[7]. Related researchers attempt to infuse intelligence into objects to learn from the physical world [8], [9]. The IoT with cognitive ability is called cognitive Internet of Things (CIoT), which enables objects and groups to learn data from connected devices, sensors, machines and other sources. Briefly, CIoT enhances the current IoT by integrating the human cognition process into the

The associate editor coordinating the review of this manuscript and approving it for publication was Min Jia.

system design. The advantages are multifold, e.g., saving people's time and effort, increasing resource efficiency, and enhancing service provisioning [10], [11].

WSN, which collects information from the users and environment while the actuators transfer the data to CIoT framework through gateway controller, is an important part of CIoT [12]. As one can imagine, objects within CIoT can understand correctly and behave appropriately only if the localization information of the sensor nodes is accurate and robust. The localization of WSNs can help establish dynamic routing, search optimal transmission path adaptively and optimize configuration of each node to improve the transmission performance of CIoT [13]. To solve the localization problem for WSN, equipping each sensor node with a GPS receiver is the most simple and precise solution [14], [15]. However, adding GPS to all nodes is not always practical because of cost, limited power, size, and work condition. A reasonable method for the problem is to make certain node called an anchor node to identify their location information through GPS or fixed positions [16]. These anchor nodes can help the location-unaware sensor nodes called unknown nodes calculate locations by assistant information of distance, RSSI, or time by broadcasting location periodically.

Based on the mobility state of anchor nodes, existing anchor nodes assisted localization schemes are generally categorized into two types: one is based on multiple stationary anchor nodes [17]–[19], and the other is based on mobile anchor node(s) [20], [21], namely the static anchor node assisted localization and the mobile anchor node assisted localization. In the former case, localization algorithms estimate the location of unknown nodes by using a priori knowledge of the absolute position of static anchor nodes and information, such as distance and bearing mechanism, connectivity between unknown nodes and anchor nodes. Static anchor node assisted localization method typically requires high anchor nodes density. In the latter case, numerous virtual anchor nodes are generated to assist localization when mobile anchor nodes move. The methods based on mobile anchor node can save the cost of deploying numerous static anchor nodes, and that the localization reliability and accuracy can be improved by planning the trajectory of the mobile anchor nodes. Our research belongs to the latter, which studies the path planning of mobile anchor node and the calculation of the unknown nodes location. In addition, classic distance measurement methods include angle of arrival (AoA), time of arrival (ToA), time difference of arrival (TDoA), and received signal strength indicator (RSSI). The first three methods often require complex hardware set up while RSSI is simpler than the others but less accurate. We chose the RSSI to estimate the unknown node location and improve the accuracy of the algorithm by the linear fitting method after gathering the information of anchor node.

The remainder of the paper is organized as follows. Section II presents the related works on mobile anchor node assisted localization algorithms. Section III describes the network model. Section IV describes the LDVSL algorithm in details. Simulation results are analyzed in section V, and conclusions are drawn in section VI.

II. RELATED WORK

Mobile anchor nodes move in a sensing area and transmit message packets with the information including coordinates and time. The unknown node receives the packets, measures a received signal strength indicator (RSSI), and calculates the distance between itself and the mobile anchor node. An important research issue of localization based on mobile anchor nodes is to design the movement of mobile anchor nodes to obtain good localization performance [22], [23].

In some research, mobile anchor nodes move among unknown nodes with mobility model without considering WSN conditions [24]–[27]. Lim *et al.* [24] use the simplest mobility model in which mobile anchor nodes move randomly. Many other mobile models such as Random Waypoint (RWP), Gauss-Markov (GM) and Group mobility model have also been used in mobile anchor node assisted localization schemes [25]–[27]. In fact, the localization schemes based on mobility model are usually limited, given that the random movement path of anchor nodes may not cover all positioning areas [28].

Numerous researchers turned their attention to localization schemes based on path planning, in which anchor nodes move along the path particularly designed for localization. In [29], Koutsonikolas *et al.* studied three trajectory trajectories, namely, Scan, Double Scan, and Hilbert for the mobile landmark. The authors analyzed the influence of anchor nodes collinearity on localization accuracy. Han *et al.* [30] proposed a localization algorithm with a mobile anchor node based on trilateration for WSNs (LMAT), in which a mobile anchor node traverses in accordance with the trilateration trajectory in the entire deployment area and broadcasts its current position periodically. An efficient energy model was proposed using breadth-first and backtracking greedy algorithms to transform the path planning problem into a spanning tree [31]. Zaidi *et al.* [32] proposed a spring swarm localization algorithm (SSLA) which uses the network topology information and a small amount of anchor node location information to calculate unknown nodes position. However, both [31] and [32] suffer from high error rate. To enable a trade-off between location accuracy and energy consumption, Han *et al.* [33] proposed a path-planning algorithm SLMAT combined of LMAT and SCAN algorithm, which ensures that each unknown node is covered by a regular triangle formed by beacons. Virtual anchor nodes compose regular triangles to solve the collinearity problem well. Rezazadeh and Moradi [34] proposed a superior path-planning algorithm for mobile anchor node-assisted localization called Z-curve, in which a path planning scheme in three-dimensional area is studied. Mobile anchor nodes form a regular tetrahedron and traverse three-dimensional region following a trajectory similar to Scan. Several methods have been proposed to introduce directional antennas to mobile anchor nodes to expand the coverage [35], [36].

An event-driven object localization method based on directional antennas was proposed for disaster rescue scenarios in [37]. Obstacle avoidance traverse is realized through a mobile anchor node with four directional antennas and a GPS module, and the locations during mobility are broadcast. This strategy allows the mobile anchor node to move along any curve path and can be utilized under the event-driven scenario to provide self-localization.

The above mentioned methods demonstrate unique advantages in their application scenarios. However, GPS devices are adopted to provide location information for mobile anchor nodes. GPS increases the cost and energy consumption of mobile node, and limits the application scenario of localization system. In this paper, we focus on the path planning of mobile anchor nodes for uniform deployment and propose a mobile anchor node Localization method based on the Diameter-Varying Spiral Line (LDVSL). Owing to the unique characteristics of the path planning, the position information of the mobile anchor node can be obtained by time and angle mechanism rather than by GPS. In addition, the maximum RSSI value is selected by the linear fitting method to improve the localization accuracy.

III. NETWORK MODEL

A. NETWORK MODEL AND REGION SEGMENTATION

The WSN to be considered consists of a number of unknown sensor nodes and one mobile anchor node. The unknown node is the node to be located. The mobile anchor node travels in the network following the path which is planned in this section. The communication radius of the mobile anchor node is R, which is adjustable. The mobile anchor node periodically sends position message packet with coordinates. We assume that the distance between the mobile anchor node and the unknown node is estimated using RSSI technique.

All unknown nodes are randomly distributed in a square region, namely, region of interest (ROI). To clearly describe the trajectory of a mobile anchor node, the ROI is divided into n equal parts, and the width of each part is equal to the communication distance of anchor node R, as illustrated in Fig. 1. The width of the ROI is denoted as L, $L = nR$.

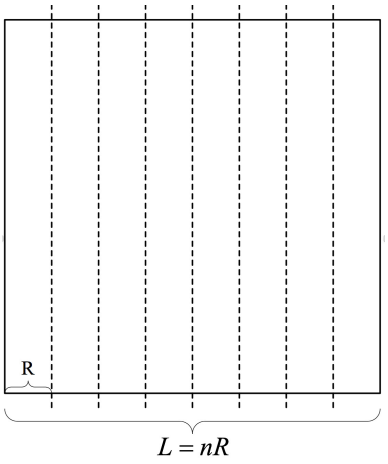

FIGURE 1. Region segmentation.

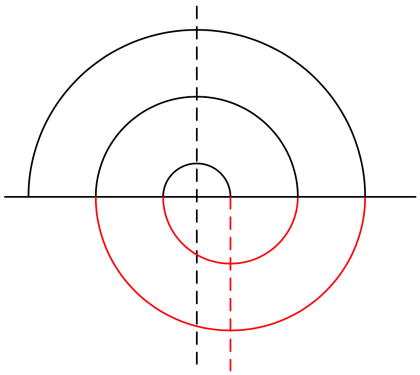

FIGURE 2. Diagram of a diameter-varying spiral line.

B. MOBILE PATH PLANNING

The classic spiral moving path is a standard Archimedean spiral, the pitch of which increases continuously. However, this moving path may make a few unknown nodes unable to be located given the change in spiral pitch. We assume that an anchor node moves along a diameter-varying spiral line, which is composed of arcs with specific angle, to solve the above mentioned problem.

It is generally considered that the spiral line and the arc are different. However, the arc with its center deviated is indeed a spiral line. An arc is a part of a circle, and the distance from any point to the center of the circle in the arc is equal, while the distance from any point to the pole of the spiral line is gradually changing. In Fig. 2, the diameter-varying spiral line extends into a spiral by increasing the radius and switching the center of arc regularly. The 180° arc is adopted here to connect the arcs smoothly. The distance between the two connected semicircles centers is R/2. The radius of arc is increased by R/2 every time. The pitch of arc is defined as the arc diameter that varied at 360°. Therefore, the pitch of the diameter-varying spiral line is constant.

Fig. 3 illustrates the path planning in accordance with the 180° diameter-varying spiral line and the distribution of nodes. The coordinate system is established in a square region of 500 m × 500 m, and the center of the area is taken as the original point. The spiral pitch is fixed and equal to the communication radius of mobile anchor node.

The mobile anchor node moves along the special diameter-varying spiral line and broadcasts its location regularly. We assume that there is a virtual anchor node in each location where the mobile anchor node broadcasts a packet. The path planning provides the opportunity for the time angle geometry method for localization.

C. DIRECTIONAL ANTENNA MODEL

An antenna is a passive device which does not offer any added power to the signal. Instead, an antenna simply redirects the energy it receives from the transmitter. The redirection has

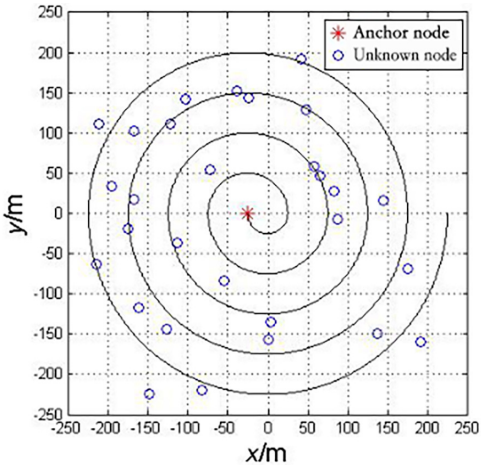

FIGURE 3. Path planning and node distribution of a diameter-varying spiral line.

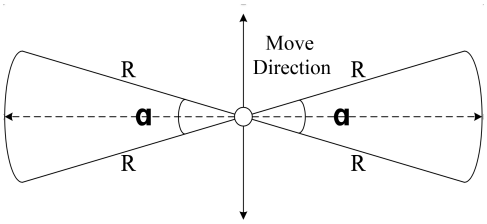

FIGURE 4. Diagram of directional antenna for mobile anchor node.

the effect of providing more energy in one direction, and less energy in all other directions. Directional antenna can divert the RF energy in a particular direction to farther distance in wireless networks. Therefore, a directional antenna can make node cover long range, while the effective beam width decreases. Directional antenna can help counteract fading and multi-path, and help cut down the loss of energy in the ineffective direction.

A directional antenna is suitable for deployment in the field environment given the superiority in high forward gain and flexible radiation angle. A bi-directional antenna is fixed to the mobile anchor node in the proposed method. The radiation pattern of directional antenna for the mobile anchor node is shown in Fig. 4, where α is the radiation angle, and R is the communication radius. The centerline of the radiation range of two directions is constantly perpendicular to the moving direction of the anchor node.

Let the mobile anchor node move along the diameter-varying spiral line from (−R/2, 0) left of the coordinate origin, as demonstrated in Fig. 3, and end at (R(n−1)/2, 0). The initial time is set as 0, and the angular velocity is a fixed value $\omega(rad/s)$. The antenna broadcasts packets periodically in two directions simultaneously. Each packet has four fields: ID, Antenna direction, Time, and Angular velocity. Antenna direction field is noted as ''left'' when the packet is transmitted by the left antenna; and noted as ''right'' when the packet is transmitted by the right antenna.

IV. LOCALIZATION METHOD USING THE DIAMETER-VARYING SPIRAL LINE

The mobile anchor node travels along the planning path and periodically broadcasts information to help unknown nodes for localization. Three assumptions are made: (a) The mobile anchor node has sufficient energy for moving and broadcasting information packets during localization. (b) The mobile anchor node has identical communication range R at all anchor points. (c) The speed of the mobile anchor node is adjustable and uniform in the process of localization.

A. LOCALIZATION PRINCIPLE

In the proposed LDVSL algorithm, we set one mobile anchor node, and let the anchor node traverse the networks along the diameter-varying spiral line mentioned above. This anchor node broadcasts information packets, including ID, Time, Antenna direction and Angular velocity periodically. The current coordinates of the mobile anchor node can be calculated by information of time and angular velocity given the characteristics of the diameter-varying spiral line. That is, the point (x, y) in the spiral line can be obtained by

$$x = \lfloor \frac{\omega \times Time}{360} \rfloor \times cos(\omega \times Time \bmod 360); \quad (1)$$

$$y = \lfloor \frac{\omega \times Time}{360} \rfloor \times sin(\omega \times Time \bmod 360), \quad (2)$$

where ω is the angular velocity, and $Time$ is the current time value.

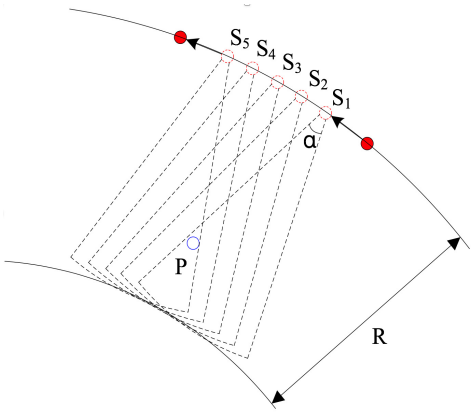

FIGURE 5. Local schematic of time and angle geometric localization mechanism.

Fig. 5 exhibits the local schematic of the time and angle geometric localization mechanism. The mobile anchor node S moves counterclockwise along a spiral line. Virtual anchor nodes are generated at the point where data packets are broadcasted. The distance between the two arcs is R, the communication radius of anchor node. S_1, S_2, S_3, S_4, S_5 are the virtual anchor nodes, which can transmit packets to the unknown node P. Here, packets are all from the left antenna of the anchor node. α is the radiation angle of a directional antenna. P is in the overlap of the communication range of multiple virtual anchor nodes. Node P is considered to locate in the

straight line from S_3 to the center point of the arc because S_3 is the middle among virtual anchor nodes. The location of P can be obtained through the distance from virtual anchor node to node P.

B. ALGORITHM LOCALIZATION PROCESS

The time and angle geometric localization mechanism based on the proposed diameter-varying spiral line in this paper can be described in detail in the four steps as follows.

1) NETWORK INITIALIZATION AND PACKETS COLLECTION

The moving path for mobile anchor node should be planned by using the diameter-varying spiral line, and the coordinate system is established, as displayed in Fig. 3. The anchor node moves and broadcasts packets periodically along the path with constant angular velocity. Simultaneously, the unknown nodes in the region will receive the packets those are broadcasted by the anchor node. Here, each point where anchor nodes send packets is recorded as a virtual anchor node.

The virtual anchor node as $S_1^{(1)}$ is denoted when the unknown node to be located receives a data packet for the first time. Moreover, its time value is recorded as $T_1^{(1)}$ and the RSSI as $RSSI_1^{(1)}$. Similarly, the virtual anchor node is recorded as $S_2^{(1)}$ when the second packet is received, and its time value is recorded as $T_2^{(1)}$ and the RSSI as $RSSI_2^{(1)}$. Repeat this process until the packet is no longer detected. The last virtual anchor node that is detected by the unknown node is recorded as $S_n^{(1)}$ with time value $T_n^{(1)}$ and the RSSI as $RSSI_n^{(1)}$. Then, we obtain the virtual anchor node set $\{S_1^{(1)}, S_2^{(1)}, \cdots, S_n^{(1)}\}$, the time value set $\{T_1^{(1)}, T_2^{(1)}, \cdots, T_n^{(1)}\}$, and the RSSI set $\{RSSI_1^{(1)}, RSSI_2^{(1)}, \cdots, RSSI_n^{(1)}\}$.

The unknown nodes outside of the diameter-varying spiral line or inside the central arc can only receive one round of data packets. However, the unknown nodes between two arcs can receive two rounds of packets from virtual anchor nodes in different arc segments. We denote another round of virtual anchor node as set $\{S_1^{(2)}, S_2^{(2)}, \cdots, S_n^{(2)}\}$. The time value and RSSI are recorded as $\{T_1^{(2)}, T_2^{(2)}, \cdots, T_n^{(2)}\}$ and $\{RSSI_1^{(2)}, RSSI_2^{(2)}, \cdots, RSSI_n^{(2)}\}$, respectively.

2) CALCULATE ANGLE OF THE VIRTUAL ANCHOR NODE IN THE MIDPOINT

If one unknown node receives two rounds of packets, the round with smaller average RSSI will be selected. The distance is extensive when the RSSI is small. Thus, numerous virtual anchor nodes that correspond to the round will be involved, and the angle will be accurate. The average RSSI of the round is denoted as

$$RSSI_{average}^{k} = \sum_{i=1}^{n} RSSI_i^k, \quad k = 1, 2., \tag{3}$$

where k represents the round number.

The midpoint of round k-th is calculated by

$$T_r^{(k)} = \begin{cases} T_{(n+1)/2}, & \text{if n is an odd integer,} \\ \dfrac{1}{2}(T_{n/2} + T_{n/2+1}), & \text{if n is an even integer.} \end{cases} \tag{4}$$

Then, the angle of the midpoint is calculated by

$$\theta_r^{(k)} = \frac{180\omega\, T_r^{(k)}}{\pi}. \tag{5}$$

3) SOLUTION TO THE MAXIMUM RSSI OF ROUND k-TH BY LINEAR FITTING

The RSSI of the midpoint is the largest because the corresponding virtual anchor node is nearest to the unknown node P. However, the broadcast period of mobile anchor node impacts the density of virtual anchor nodes. This mobile anchor node may not send a packet in the point that corresponds to $\theta_r^{(k)}$, and the detected RSSI set may not contain the corresponding RSSI value of $\theta_r^{(k)}$. Based on the fading model of RSSI [38], the relation between RSSI and distance is linear in local. The two RSSI sets are fitted to two intersecting lines. The RSSI is less than 0, and the fitting lines should be in the fourth quadrant. We opt to demonstrate linear fitting in the firstquadrant to observe conveniently.

In Fig. 6, L_1 and L_2 are two fitting lines in the coordinates that consider time as the X-coordinate and RSSI as the Y-coordinate. The intersection of two lines exhibits the maximum RSSI, which is denoted as $RSSI_{max}$; we also denote the vertical ordinate of the intersection point as $RSSI_{max}$. In Fig. 6(a), $RSSI_3$ is the nearest to $RSSI_{max}$ among the RSSI values that correspond to $\{T_1, T_2, T_3, T_4\}$ and is on a straight line L_2. In Fig. 6(b), $RSSI_2$ is the nearest to $RSSI_{max}$ and is on a straight line L_1. Obviously, no virtual anchor node presents at the intersection point. Therefore, the actual maximum RSSI that corresponds to the virtual anchor node is typically not equal to $RSSI_{max}$, and remains uncertain. If the time value that corresponds to the actual maximum RSSI is on the left of the time value of the intersection point, then the actual maximum RSSI is on the fitting line L_1, similar to Fig. 6(b). Otherwise, the actual maximum RSSI is on line L_2. The least squares method is selected to fit two sets of coordinate points, which are represented by $(T_i^j, RSSI_i^j)$. For $j = 1, 2$, the left and right points of the max RSSI are denoted, respectively. For $i = 1, 2, 3, \cdots, n$, n coordinate points are denoted. Then, we obtain the fitting lines L_1 and L_2, which are expressed as

$$RSSI^{(1)} = a_1 + k_1 T^{(1)}; \tag{6}$$

$$RSSI^{(2)} = a_2 + k_2 T^{(2)}. \tag{7}$$

The time point corresponds to max RSSI is T_f, and the fitting errors are calculated by

$$\begin{cases} e_1 = \sum (RSSI_i - k_1 T_i - a_1)^2, & i = 1, \cdots, f, \\ e_2 = \sum (RSSI_i - k_2 T_i - a_2)^2, & i = f+1, \cdots, n. \end{cases} \tag{8}$$

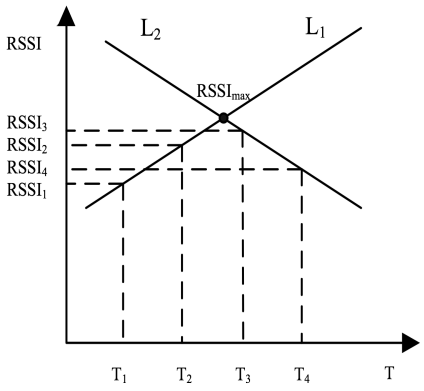

(a)

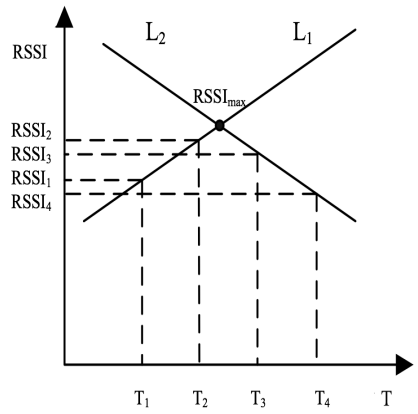

(b)

FIGURE 6. Schematic of the RSSI linear fitting. (a) Actual maximum RSSI corresponds to L_2. (b) Actual maximum RSSI corresponds to L_1.

Partial derivatives of e with respect to k and a are calculated by

$$\begin{cases} \frac{\partial e}{\partial k} = 2\sum(RSSI_i - kT_i - a)(-T_i) = 0, \\ \frac{\partial e}{\partial a} = -2\sum(RSSI_i - kT_i - a) = 0. \end{cases} \tag{9}$$

Then, the equation set of k and a is obtained by

$$\begin{cases} (\sum T_i^2)k + (\sum T_i)a = \sum RSSI_i T_i, \\ (\sum T_i)k + fa = \sum RSSI_i. \end{cases} \tag{10}$$

Let $A = \sum T_i^2, B = \sum T_i, C = \sum RSSI_i T_i, D = \sum RSSI_i$, and equation (10) can be transformed to

$$\begin{cases} Ak + Ba = C, \\ Bk + fb = D. \end{cases} \tag{11}$$

Then, k and a can be calculated by

$$\begin{cases} k = (Cf - BD)/(Af - BB), \\ a = (AD - CB)/(Af - BB). \end{cases} \tag{12}$$

We obtain the vertical ordinate of intersection of lines L_1, L_2, and $RSSI_{max}$ as follows:

$$RSSI_{max} = \frac{k_1(a_2 - a_1)}{k_1 - k_2} + a_1. \tag{13}$$

4) CALCULATE THE COORDINATES OF THE UNKNOWN NODE

$RSSI_{max}$ should be substituted into the RSSI-based distance-estimated model because the angle of the midpoint virtual anchor node $\theta_r^{(k)}$ and the corresponding $RSSI_{max}$ have been obtained. The RSSI is denoted by

$$RSSI = PL(d_0) + 10nlog(\frac{d}{d_0}) + X_\delta, \tag{14}$$

where $PL(d_0)$ is the received signal intensity at distance d_0, which is typically set to 1 m. n is the path loss exponent between 2 and 5. X_δ is the random Gauss distribution with mean zero and refers to the influence of the surrounding environment on the signal measurement. Thus, we obtain the distance d between the virtual anchor and the unknown node to be located at the moment with respect to the $RSSI_{max}$.

The unknown node is inside the virtual anchor node, $d_r = -d$, when the node receives only one round packet and the antenna direction of the packet field is ''left''. If the antenna direction of the packet field is ''right'', then the unknown node is outside the virtual anchor node, $d_r = d$.

The k-th round with a small average RSSI is selected when the unknown node receives two rounds of packets. Then, we obtain the following equation:

$$d_r = \begin{cases} -d, & Antennadirection = left, \\ d, & Antennadirection = right. \end{cases} \tag{15}$$

The coordinates of unknown node p_i are set to (x_i, y_i), and the radius of the arc in which the set coordinates are located is

$$r = R \cdot m/2 + d, \tag{16}$$

where $m = [\frac{\theta_r^{(k)}}{180}] + 1$. Then, the coordinates of unknown node p_i can be calculated by

$$(x_i, y_i) = \begin{cases} (-r \cdot cos\theta_r^k, -r \cdot sin\theta_r^k), & \text{m is odd}, \\ (-r \cdot cos\theta_r^k - R/2, -r \cdot sin\theta_r^k), & \text{m is even}. \end{cases} \tag{17}$$

Thus, we obtain location of the unknown node. Loop execution is performed until all unknown nodes are located.

V. PERFORMANCE SIMULATIONS

Our simulations were performed with MATLAB 7.0 platform. For clarity, the proposed method is noted as the LDVSL. We compared our LDVSL scheme with the following three localization schemes: a) Double Scan scheme, where the collinearity problem is overcome by the anchor node that moves in the horizontal and vertical directions, b) Hilbert scheme [29], where the model enables the unknown nodes to receive the non-collinear virtual beacon

signals directly and obtain precise estimated coordinates, and c) SLMAT scheme [35], which is a path-planning algorithm combining a localization algorithm with a mobile anchor node based on trilateration and SCAN algorithm. SLMAT ensures that each unknown node is covered by a regular triangle formed by beacons. To the best of our knowledge, Double Scan and Hilbert are the classic localization schemes, and SLMAT is the latest localization scheme under the same scenario of the proposed scheme. We implemented five sets of simulations. In subsection A and B, the performance of the proposed algorithm is evaluated and compared with Double Scan, Hilbert and SLMAT in accordance with the average localization error under two factors, including broadcast period and antenna angle. In subsection C, we analyzed the effects of the interaction of broadcast period and antenna angle on the performance of the proposed algorithm. Subsection D presents the impact of unknown node number on average localization error. We observe the impact of obstacles on average localization error in subsection E. In subsection F, we compare the average runtime per unknown node of LDVSL, Double Scan, Hilbert and SLMAT localization algorithms to observe the energy cost.

TABLE 1. Simulation parameters.

Parameter	Value
Region of network	$500\ m \times 500\ m$
Region of nodes arrangement	$400\ m \times 400\ m$
Number of unknown nodes	100
Angular velocity	$\pi/36(rad/s)$
Communication radius of anchor node	$50\ m$
Initial location of anchor node	$(-25, 0)$
Radiation angle of directional antenna	$(30, 90)$
Final location of anchor node	$(225, 0)$
Broadcasting period	$(0.5\ s, 3\ s)$
Frame length of packet field	$4000\ bits$

The deployment area is set to $500\,m \times 500\,m$. The unknown nodes are randomly distributed in the middle $400\ m \times 400\ m$ of the deployment area given that blind coverage may be located at the edge of the area. The initial position of the mobile anchor node is $(-25, 0)$. This node moves at a fixed angular velocity ω. The signal fading model is in accordance with [29], where, $P_T = -5\,dBm$, $PL(D_0) = 55\,dBm$, and $\eta = 4$ (outdoor). The mean value and variance of X_σ correspond to 0 and 5. Other main parameters are listed in Table 1. A total of 100 Monte Carlo are performed for each set of simulations to ensure the reliability of the simulation results.

A. IMPACT OF BROADCAST PERIOD ON AVERAGE LOCALIZATION ERROR

Average localization error is a basic and important index for evaluating an algorithm. This index refers to the Euclidean distance between the estimated and the real positions [39]. The actual and estimation coordinates of the unknown node are denoted by (x_i, y_i) and $(\hat{x}_i, \hat{y}_i)$, respectively. The number of unknown nodes is N, and the communication radius of the anchor node is R. The average localization error can be calculated by

$$averageerror = \frac{\sum_{i=1}^{N} \sqrt{(x_i - \hat{x}_i)^2 + (y_i - \hat{y}_i)^2}}{N}. \quad (18)$$

If the broadcast period is 1 s, the mobile anchor node broadcasts its coordinates once a second, and the production frequency of virtual anchor nodes is also once a second. We obtain additional virtual anchor nodes when the period is small. We demonstrate the changes in the average localization errors of Double Scan, Hilbert, SLMAT and the LDVSL algorithm with different broadcast periods to verify the improvement of our algorithm in terms of location accuracy and analyze the impact of the broadcast period. We set the antenna angle to 60°. In Fig. 7, the average localization errors of the four methods increase obviously while the broadcast period increases from 0.5 s to 3 s. However, the average localization error of the LDVSL is constantly the lowest among four algorithms. The average localization errors of the LDVSL are 78%, 83.1% and 91.5% of the Hilbert, Double Scan and SLMAT correspondingly, when the broadcast period is 2 s. Therefore, the proposed LDVSL improves the average localization accuracy of unknown nodes.

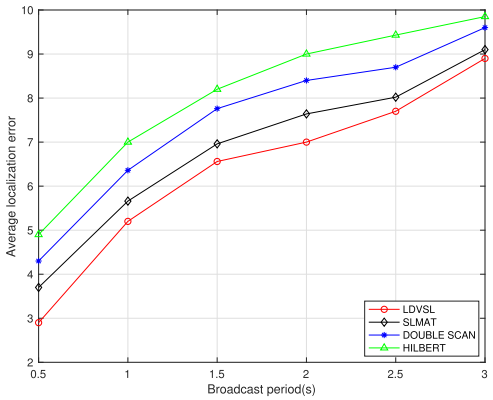

FIGURE 7. Impact of broadcast period on average localization error of different algorithms.

B. IMPACT OF ANTENNA ANGLE ON AVERAGE LOCALIZATION ERROR

In this subsection, we aim to observe the performance of the different algorithms when antenna angle changes. The broadcast period is set to 1 s. In Fig. 8, we compared the average localization errors of Double Scan, Hilbert, SLMAT and the proposed algorithm while the antenna angle changes from 30° to 90°. The average localization errors of the four algorithms increase while the antenna angles enlarge because the unknown node P is consistently within the overlap of the communication range of multiple virtual anchor nodes. A larger range will lead to a reduction in precision. However, the average localization error of the proposed algorithm is lower than the three other methods regardless of the antenna angle.

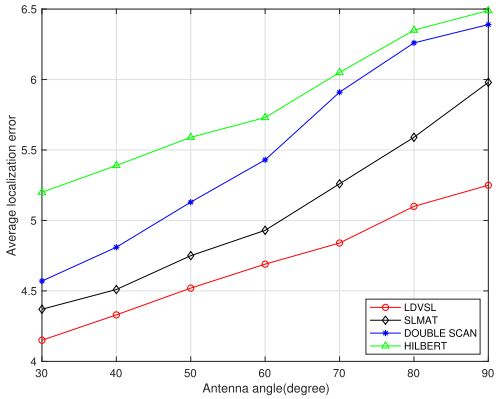

FIGURE 8. Impact of antenna angle on average localization error of different algorithms.

C. INTERACTION IMPACT OF BROADCAST PERIOD AND ANTENNA ANGLE ON THE PERFORMANCE OF LDVSL

In this subsection, the performance of the proposed algorithm is evaluated in accordance with the average localization error and positionable node ratio (PNR) under different combinations of antenna angle and broadcast period. The PNR refers to the proportion of the number of unknown nodes below a given average error threshold to the total number of unknown nodes.

We have observed the impact of their different combinations on the PNR in Fig. 9(a). The PNR performs well and is above 96.1% when the broadcast period is 0.5 s, or when the broadcast period is 1 s or 1.5 s and the antenna angle is larger than 60°. The PNR of a 2 s broadcast period at 30° of the antenna angle is only 69.1%. The average localization error deteriorates seriously to 13.9, although the PNR of a 2 s broadcast period can reach 92% with the increase in antenna angle, as depicted in Fig. 9(b).

Furthermore, shown as Fig.10(a) and Fig.10(b), two three-dimensional diagrams are given to illustrate the trend of average localization error and PNR changing with two parameters (broadcast period and antenna angle) simultaneously. In order to give macroscopic diagrams of parameters variations, we adjust broadcast period range from 0.5 to 3 and antenna angle range from 20 to 100.

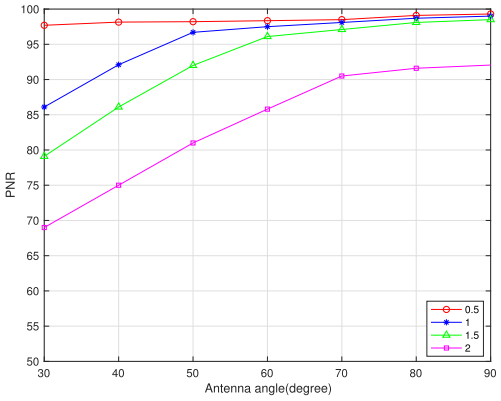

(a)

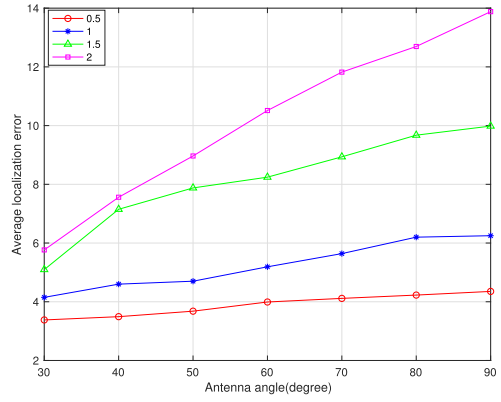

(b)

FIGURE 9. Interaction impact of broadcast period and antenna angle on performance of LDVSL. (a) Interaction impact on the PNR. (b) Interaction impact on the average localization error.

D. IMPACT OF UNKNOWN NODE NUMBER ON AVERAGE LOCALIZATION ERROR

To observe the impact of unknown node number on average localization error, we conduct a set of simulation experiments by considering the antenna angle of 50° and broadcast period of 0.5 s as simulation parameters. We set two unknown nodes randomly at 400 $m \times 400$ m of the deployment area initially and then add two nodes in each round until the number becomes 100 to observe the effects of the unknown node number in the deployment area on the performance of the proposed algorithm. Five simulations are performed for each round to obtain an average localization error, and there are 5×50 rounds in total. In Fig. 11, the average localization error has a slight uptrend overall. However, the average localization error only slightly changed when the number of the unknown nodes increases. The variation of the unknown node number has a minimal influence on the average localization error of the proposed algorithm, thereby indicating that the proposed algorithm is robust to the change in the unknown node number.

E. IMPACT OF OBSTACLES ON AVERAGE LOCALIZATION ERROR

Experiments discussed above are carried out without obstacles. However, if there exist nodes or obstacles between the unknown node and the anchor node, the RSSI value received by the unknown node will be smaller than it should be. Since it is difficult to guarantee the proportion of anchor nodes affected by randomly setting obstacles, we decrease a certain proportion of the RSSI values from RSSI value set acquired by the unknown node mentioned in section IV-B. In Fig. 12, we compare the variation of average localization errors of Double Scan, Hilbert, SLMAT and the proposed algorithm when the ratio of abnormal RSSI changes from

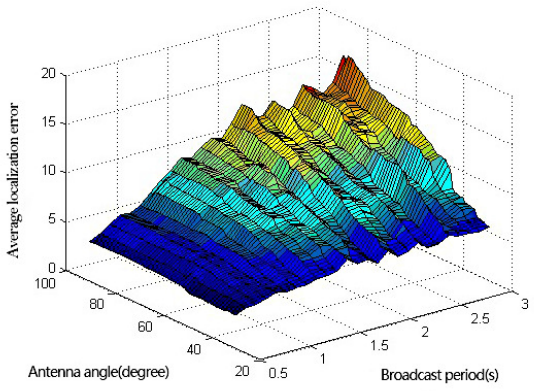

(a)

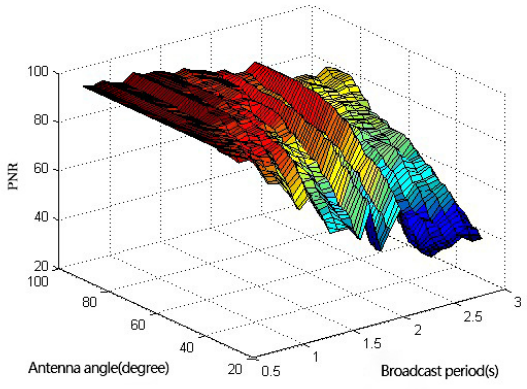

(b)

FIGURE 10. Trend of average localization error and PNR changing with broadcast period and antenna angle. (a) Trend of average localization error. (b) Trend of PNR.

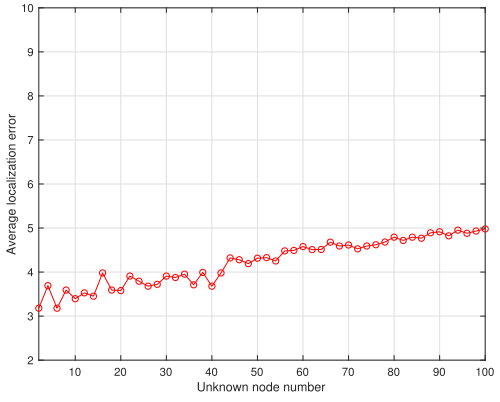

FIGURE 11. Impact of unknown node number on average localization error.

0 to 30 percent. It is found that the average localization error of the proposed algorithm varies from 3.237 to 3.762 and is not significantly affected by obstacles when the ratio is less than 10 percent. It is obviously more desirable than the other three schemes. However, when the ratio is larger than 10 percent, average localization errors of all four schemes

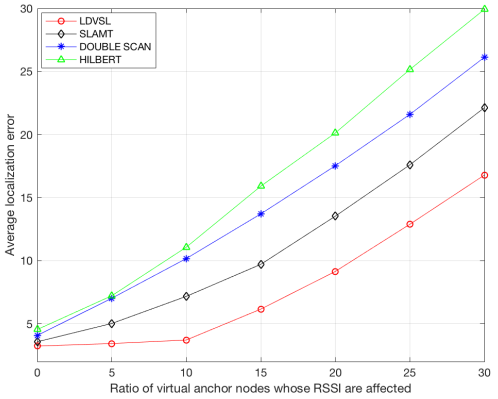

FIGURE 12. Impact of obstacles on average localization error.

TABLE 2. Comparison of computational runtime among different localization algorithms.

Algorithms	LDVSL	Double Scan	Hilbert	SLMAT
$with\ obstacles(\mu s)$	1654	9500	12690	23960
$without\ obstacles(\mu s)$	2980	11460	16650	34700

deteriorated seriously. The proposed algorithm can get over the impact of the obstacles to some extent. There are two reasons. First, as mentioned in part IV-B, the ''round'' with a small average RSSI will be selected to satisfy the calculation. The round selection is based on the average value of a set of RSSI received by unknown node, rather than single RSSI value, so the round selected is not affected seriously by single RSSI value; second, the virtual anchor node whose RSSI is decreased will induce a noise point in linear fitting. The linear fitting method can measure the distance between the fitting line and the noise point inherently, and remove the point corresponding to the abnormal RSSI.

F. COMPUTATIONAL RUNTIME

In addition, we compared the average computational runtime per unknown node of LDVSL, Double Scan, Hilbert and SLMAT localization algorithms with and without obstacles influence. The average computational runtime is the average CPU time for locating one unknown node. All runtime data is provided in Table 2. Due to the unique characteristics of the diameter-varying spiral line and efficient linear fitting, the proposed algorithm has an overwhelmingly less CPU runtime when compared to three competing algorithms, regardless of whether there are obstacles. Therefore, the computational load of the proposed algorithm is obviously the lowest. The proposed algorithm is promising to be solidified as a novel low energy cost technique.

VI. CONCLUSIONS

Many intelligent applications in Cognitive Internet of Things depend on devices being able to accurately determine their locations. For WSN, we propose a mobile anchor node

assisted localization algorithm based on the diameter-varying spiral line (LDVSL), in which the virtual anchor node position is obtained by time and angle mechanism instead of GPS given the unique path characteristics of the mobile anchor node. The simulation results indicate that LDVSL algorithm outperforms Double Scan, Hilbert and SLMAT algorithms in terms of average localization error. Moreover, we analyzed the influence of broadcast period and antenna angle on the performance of the LDVSL algorithm in terms of PNR and average localization error. The proposed algorithm exhibits high accuracy, excellent coverage probability, and good robustness under the premise of favorable parameters.

REFERENCES

[1] M. Jia, X. Gu, Q. Guo, W. Xiang, and N. Zhang, "Broadband hybrid satellite-terrestrial communication systems based on cognitive radio toward 5G," *IEEE Wireless Commun.*, vol. 23, no. 6, pp. 96–106, Dec. 2016.

[2] M. Jia, X. Liu, X. Gu, and Q. Guo, "Joint cooperative spectrum sensing and channel selection optimization for satellite communication systems based on cognitive radio," *Int. J. Satell. Commun. Netw.*, vol. 35, no. 2, pp. 139–150, 2017.

[3] M. Jia, Z. Yin, Q. Guo, G. Liu, and X. Gu, "Waveform design of zero head DFT spread spectral efficient frequency division multiplexing," *IEEE Access*, vol. 5, pp. 16944–16952, 2017.

[4] Y. Tu, Y. Lin, J. Wang, and J.-U. Kim, "Semi-supervised learning with generative adversarial networks on digital signal modulation classification," *Comput. Mater. Continua*, vol. 55, no. 2, pp. 243–254, 2018.

[5] Y. Lin, Y. Li, X. Yin, and Z. Dou, "Multisensor fault diagnosis modeling based on the evidence theory," *IEEE Trans. Rel.*, vol. 67, no. 2, pp. 513–521, Jun. 2018.

[6] J. Sun *et al.*, "A multi-focus image fusion algorithm in 5G communications," *Multimedia Tools Appl.*, no. 3, pp. 1–20, Dec. 2018.

[7] Y. Lin, X. Zhu, Z. Zheng, and R. Zhou, "The individual identification method of wireless device based on dimensionality reduction and machine learning," *J. Supercomput.*, pp. 1–18, Dec. 2017. doi: 10.1007/s11227-017-2216-2.

[8] Y. Lin, C. Wang, J. Wang, and Z. Dou, "A novel dynamic spectrum access framework based on reinforcement learning for cognitive radio sensor networks," *Sensors*, vol. 16, no. 10, p. 1675, 2016.

[9] T. Wang, Z. Zheng, Y. Lin, S. Yao, and X. Xie, "Reliable and robust unmanned aerial vehicle wireless video transmission," *IEEE Trans. Rel.*, to be published. doi: 10.1109/TR.2018.2864683.

[10] T. Wang, Z. Zheng, M. H. Rehmani, S. Yao, and Z. Huo, "Privacy preservation in big data from the communication perspective—A survey," *IEEE Commun. Surveys Tuts.*, vol. 21, no. 1, pp. 753–778, 1st Quart., 2018.

[11] Z. Zheng, A. K. Sangaiah, and T. Wang, "Adaptive Communication Protocols in Flying Ad Hoc Network," *IEEE Commun. Mag.*, vol. 56, no. 1, pp. 136–142, Jan. 2018.

[12] X. Shi *et al.*, "Graph processing on GPUs: A survey," *ACM Comput. Surv.*, vol. 50, no. 6, p. 81, 2018.

[13] Z. Zheng, N. Saxena, K. K. Mishra, and A. K. Sangaiah, "Guided dynamic particle swarm optimization for optimizing digital image watermarking in industry applications," *Future Gener. Comput. Syst.*, vol. 88, no. 11, pp. 92–106, 2018.

[14] A. Alomari, F. Comeau, W. Phillips, and N. Aslam, "New path planning model for mobile anchor-assisted localization in wireless sensor networks," *Wireless Netw.*, vol. 28, no. 7, pp. 2589–2607, 2018.

[15] H. Qu, G. Hou, Y. Guo, N. Wang, and Z. Guo, "Localization with single stationary anchor for mobile node in wireless sensor networks," *Int. J. Distrib. Sensor Netw.*, vol. 9, no. 4, 2013, Art. no. 212806.

[16] C.-H. Ou and W.-L. He, "Path planning algorithm for mobile anchor-based localization in wireless sensor networks," *IEEE Sensors J.*, vol. 13, no. 2, pp. 466–475, Feb. 2013.

[17] C.-T. Chang, C.-Y. Chang, and C.-Y. Lin, "Anchor-guiding mechanism for beacon-assisted localization in wireless sensor networks," *IEEE Sensors J.*, vol. 12, no. 5, pp. 1098–1111, May 2012.

[18] T. Kim, M. Shon, M. Kim, D. S. Kim, and H. Choo, "Anchor-node-based distributed localization with error correction in wireless sensor networks," *Int. J. Distrib. Sensor Netw.*, vol. 8, no. 4, 2012, Art. no. 975147.

[19] X. Chen, J. Chen, J. He, and B. Lei, "An improved localization algorithm for wireless sensor network based on the selection of benchmark anchor node," *J. Netw.*, vol. 7, no. 6, p. 991, 2012.

[20] Z.-H. Qian and Y.-J. Wang, "Internet of Things-oriented wireless sensor networks review," *J. Electron. Inf. Technol.*, vol. 35, no. 1, pp. 215–227, 2013.

[21] S. Halder and A. Ghosal, "A survey on mobile anchor assisted localization techniques in wireless sensor networks," *Wireless Netw.*, vol. 22, no. 7, pp. 2317–2336, 2016.

[22] Q. I. A. N. Zhihong, S. U. N. Dayang, and V. Leng, "A survey on localization model in wireless networks," *Chin. J. Comput.*, vol. 39, no. 6, pp. 1237–1256, 2016.

[23] C.-C. Chen and T.-C. Lin, "A low-cost anchor placement strategy for range-free localization problems in wireless sensor networks," *Int. J. Distrib. Sensor Netw.*, vol. 19, no. 12, 2013, Art. no. 782451.

[24] S. Lim, C. Yu, and C. R. Das, "A realistic mobility model for wireless networks of scale-free node connectivity," *Int. J. Mobile Commun.*, vol. 8, no. 3, pp. 351–369, May 2010.

[25] C.-H. Ou, K.-F. Ssu, and H. C. Jiau, "Range-free localization with aerial anchors in wireless sensor networks," *Int. J. Distrib. Sensor Netw.*, vol. 2, no. 1, pp. 1–21, 2006.

[26] C.-H. Ou and K.-F. Ssu, "Sensor position determination with flying anchors in three-dimensional wireless sensor networks," *IEEE Trans. Mobile Comput.*, vol. 7, no. 9, pp. 1084–1097, Sep. 2008.

[27] B. Xiao, H. Chen, and S. Zhou, "Distributed localization using a moving beacon in wireless sensor networks," *IEEE Trans. Parallel Distrib. Syst.*, vol. 19, no. 5, pp. 587–600, May 2008.

[28] G. Han, J. Jiang, C. Zhang, T. Q. Duong, M. Guizani, and G. Karagiannidis, "A survey on mobile anchor node assisted localization in wireless sensor networks," *IEEE Commun. Surveys Tuts.*, vol. 18, no. 3, pp. 2220–2243, 3rd Quart., 2016.

[29] D. Koutsonikolas, S. M. Das, and Y. C. Hu, "Path planning of mobile landmarks for localization in wireless sensor networks," *Comput. Commun.*, vol. 30, no. 3, pp. 2577–2592, 2007.

[30] G. Han, H. Xu, J. Jiang, L. Shu, T. Hara, and S. Nishio, "Path planning using a mobile anchor node based on trilateration in wireless sensor networks," *Wireless Commun. Mobile Comput.*, vol. 13, no. 14, pp. 1324–1336, 2014.

[31] S. Zhang, J. Cao, C. Li-Jun, and D. Chen, "Accurate and energy-efficient range-free localization for mobile sensor networks," *IEEE Trans. Mobile Comput.*, vol. 9, no. 6, pp. 897–910, Jun. 2010.

[32] S. Zaidi, A. El Assaf, S. Affes, and N. Kandil, "Range-free nodes localization in mobile wireless sensor networks," in *Proc. IEEE ICUWB*, Montreal, QC, Canada, Oct. 2015, pp. 1–6.

[33] G. Han, X. Yang, L. Liu, M. Guizani, and W. Zhang, "A disaster management-oriented path planning for mobile anchor node-based localization in wireless sensor networks," *IEEE Trans. Emerg. Topics Comput.*, to be published. doi: 10.1109/TETC.2017.2687319.

[34] J. Rezazadeh, M. Moradi, A. S. Ismail, and E. Dutkiewicz, "Superior path planning mechanism for mobile beacon-assisted localization in wireless sensor networks," *IEEE Sensors J.*, vol. 14, no. 9, pp. 3052–3064, Sep. 2014.

[35] Y. Fu, "Single anchor node real-time positioning algorithm based on the antenna array," *Int. J. Distrib. Sensor Netw.*, vol. 13, no. 5, pp. 1–13, 2017.

[36] Y. Ding, C. Wang, and L. Xiao, "Using mobile beacons to locate sensors in obstructed environments," *J. Parallel Distrib. Comput.*, vol. 70, no. 6, pp. 644–656, Jun. 2010.

[37] A. Alomari, W. Phillips, N. Aslam, and F. Comeau, "Dynamic fuzzy-logic based path planning for mobility-assisted localization in wireless sensor networks," *Sensors*, vol. 17, no. 8, pp. 1904–1930, Aug. 2017.

[38] Q. Hu, L. Wu, C. Cao, and S. Zhang, "An event-driven object localization method assisted by beacon mobility and directional antennas," *Int. J. Distrib. Sensor Netw.*, vol. 11, no. 6, 2015, Art. no. 134964.

[39] G. Wang, H. Chen, Y. Li, and M. Jin, "On received-signal-strength based localization with unknown transmit power and path loss exponent," *IEEE Wireless Commun. Lett.*, vol. 1, no. 5, pp. 536–539, Oct. 2012.

XIN WANG received the B.E. degree in electronic and information engineering and the M.E. degree in signal and information processing from the Changchun University of Technology, China, in 2003 and 2005, respectively. She is currently pursuing the Ph.D. degree with the College of Communication Engineering, Jilin University, China. She is currently an Associate Professor with the College of Information Technology, Jilin Agricultural University, China. Her research interests include device-to-device communication and wireless sensor networks.

ZHIHONG QIAN (SM'12) received the Ph.D. degree in communication and information systems from Jilin University, China, in 2001. Since 2004, he has been a Professor with the Department of Communication Engineering, Jilin University. His research interests include wireless sensor networks, the theory and applications of the Internet of Things based on Bluetooth, Zigbee, and RFID technologies, and device-to-device communication. He is a Senior Member of the Chinese Institute of Electronics and the Institute of Communications. He is also a Member of the Electronic Circuit and System Council of the Chinese Institute of Electronics, the IEEE Harbin Section Chapter Communications Society in China, and the National Higher Education Teaching Guidance Committee for Internet of Things. He is an Editorial Board Member of the *Journal of Communications*, the *Journal of Electronics and Information Technology*, the *Journal of Electronics*, the *Chinese Journal of Electronics*, and the *China Communications*.

XUE WANG received the M.E. and Ph.D. degrees in communication and information systems from Jilin University, China, in 2009 and 2012, respectively, where she has been an Associate Professor with the Department of Communication Engineering, since 2014. Her research interests include ultra wide-band, wireless network communication systems, radio frequency identification, and the Internet of Things.

LAN HUANG received the B.E., M.E., and Ph.D. degrees from Jilin University, China, in 1994, 1999, and 2003, respectively, all in computer application technology, where she is currently a Professor with the College of Computer Science and Technology. Her research interests include data mining and data warehousing. She is a Senior Member of the China Computer Federation.